

Analysis of Elastic Scattering of α Particles on $^{90,91}\text{Zr}$ Targets at Different Energy

Amane I. Istaiti

Applied Sciences Private University, Amman, Jordan

Abstract: The analysis of angular distributions of two elastic scattering processes $^4\text{He}+^{90}\text{Zr}$ (at laboratory energies 21, 23 and 25 MeV) and $^4\text{He}+^{91}\text{Zr}$ (at laboratory energies 21, 23.4 and 25 MeV) using semi classical model based on strong absorption phenomenon. The parameterized scattering matrix of McIntyre Model and Regge pole model are used to reproduce the cross-sections of the experimental data for the two elastic scattering processes at forward and backward angles. Some geometrical parameters are extracted for colliding nuclei together with total reaction cross sections.

Key words: Heavy-ion scattering, strong absorption model, McIntyre plus regge models pole model, cross-sections, experimental data, colliding nuclei

INTRODUCTION

In most of nuclear mechanisms, the incident nucleus is strongly absorbed upon entering the target nucleus where some particles of incident nucleus may be removed in semi classical models, the analysis of such elastic scattering data is conducted in terms of the asymptotic properties of the scattered wave function. These semi classical models can be compared with the potential model where the assumptions consider an average nuclear potential in which the absorption, they enable us to analyze the experimental data of elastic scattering directly and in a terms of a minimum number of parameters (Badran and Masri, 2013). This research proposes to analyze the experimental data of angular distribution for elastic scattering of α particles from target $^{90,91}\text{Zr}$ at different laboratory energy using the McIntyre plus Regge models. The analysis will be start the numerical method based on parameterizations of scattering matrix elements and based on Strong Absorption Model (SAM). This analysis will explain the diffractive condition, several parameters extract from models employed as fixed entries in the fitting process for forward angel and backward angel of angular distribution (Badran *et al.*, 2010).

MATERIALS AND METHODS

Theory: The amplitude $f(\theta)$ as a function of partial wave expansion for elastic scattering shown by:

$$f(\theta) = \frac{1}{i2k} \sum_{\ell=0}^{\infty} (2\ell+1) [S_{\ell}-1] P_{\ell}(\cos \theta) \quad (1)$$

Where:

S_{ℓ} = The complex amplitude of the ℓ th scattered partial wave

$P_{\ell}(\cos \theta)$ = The Legendre polynomial of order ℓ and k is the wave number

The scattering matrix amplitude is express by:

$$S_{\ell} = \eta_{\ell} e^{2i\delta_{\ell}} \quad (2)$$

The Coulomb phase shifts are given by the exact solution of the Rutherford scattering problem:

$$\sigma_{\ell} = \arg \Gamma(\ell+1+i\eta) \quad (3)$$

The semi-classical strong absorption model has the sharp cutoff Eq. 1 and 3:

$$\begin{aligned} \eta_{\ell} &= 0 & S_{\ell} &= 0 & \text{if } \ell \leq \ell_g \\ \eta_{\ell} &= 1 & S_{\ell} &= e^{(2i\sigma_{\ell})} & \text{if } \ell > \ell_g \end{aligned} \quad (4)$$

Here η_{ℓ} is called the reflection coefficient of the outgoing ℓ th partial wave determined by the boundary conditions at the nuclear surface. This means that waves up to the grazing angular momentum ℓ_g are completely absorbed, The sum of radii R of the projectile R_p and target nuclei R_T . This strong interaction radius has been defined:

$$R = r_0 (A_p^{1/3} + A_T^{1/3}) \quad (5)$$

Regge-pole factor expressed as:

$$S(\ell) = \left[1 + e^{-i\alpha} e^{(\ell - \ell_0)/\Delta} \right]^{-1} \left[1 + \frac{\ell - \ell_0 - iZ(\ell)}{\ell - \ell_0 - i\Gamma(\ell)/2} \right]$$

Or

$$S(\ell) = \left[1 + e^{-i\alpha} e^{(\ell - \ell_0)/\Delta} \right]^{-1} \left[1 + \frac{iD(\ell)}{\ell - \ell_0 - i\Gamma(\ell)/2} \right]$$

The $z(\ell)$ and $p(\ell)$ functions in equation, represent the Regge zero and Regge pole at a complex^l (Badran *et al.*, 2015). Where amplitude of the pole is:

$$D(\ell) = D_0 [1 - \text{Re } S_\ell(\text{BG})]$$

And the width of the pole is $\Gamma(\ell) = \Gamma_0 [1 - \text{Re } S_\ell(\text{BG})]$
 The phase of the pole is represented by ϕ^l (Badran *et al.*, 2010, 2015; Badran and Masri, 2013; Badran and Istiti, 2016; Amane, 2018).

RESULTS AND DISCUSSION

The available experimental data of scattering ^4He by different target nuclei $^{90}\text{Zr}, ^{91}\text{Zr}$ are analyzed using the combined model of McIntyre and Regge by fitting the calculated results to the experimental data. We obtain the best fit of experiment data of angular distribution and the final choice of extracted parameters depend on the smallest value of χ^2 , the seven parameters inputs $r_0, d, \mu_M, D_0, \Gamma_0, \ell_0$, and $\phi \ell_0$, to get the best fitting (Istiti, 2018).

Elastic scattering of $^4\text{He} + ^{90,91}\text{Zr}$ target nuclei: McIntyre plus Regge pole are used to analyze the experimental data of angular distribution for elastic scattering of a particle by target nuclei $^4\text{He} + ^{90}\text{Zr}$ (at laboratory energies 21, 23 and 25 MeV) and $^4\text{He} + ^{91}\text{Zr}$ (at laboratory energies 21, 23.4 and 25 MeV) using combined model of McIntyre and Regge Model (solid line) as shown in Fig. 1 (Table 1).

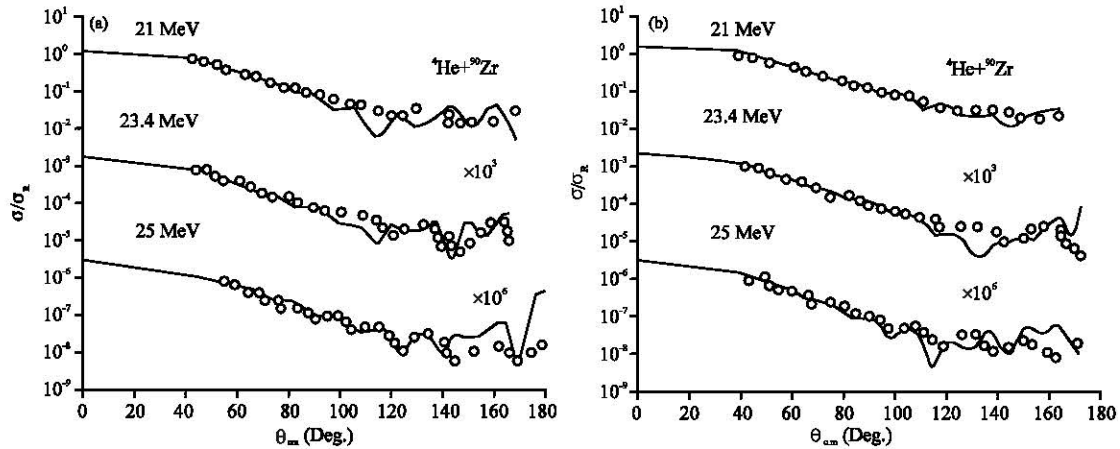


Fig. 1: The experimental data (symbols) of angular distribution of elastic scattering of α particles by the target nuclei: a) ^{90}Zr (at laboratory energies 21, 23 and 25 MeV) and b) ^{91}Zr (at laboratory energies 21, 23.4 and 25 MeV) using Regge pole model (solid line)

Table 1: List of parameters for elastic scattering of α particles by the target nuclei, ^{90}Zr (at laboratory energies 21, 23 and 25 MeV) and ^{91}Zr (at laboratory energies 21, 23.4 and 25 MeV) using Regge pole model. The total reaction cross sections σ_r (FM) and σ_r (GFM) are obtained from Fresnel Model (FM) and Generalized Fresnel Model (GFM), respectively

Elastic scattering	$^4\text{He} + ^{90}\text{Zr}$	$^4\text{He} + ^{90}\text{Zr}$	$^4\text{He} + ^{90}\text{Zr}$	$^4\text{He} + ^{90}\text{Zr}$	$^4\text{He} + ^{90}\text{Zr}$	$^4\text{He} + ^{90}\text{Zr}$
E_{Lab} (MeV)	25	23.4	21	25	23	21
r_0 (fm)	1.30	1.39	1.47	1.36	1.40	1.45
μ (Rad)	0.295	0.27	0.25	0.38	0.22	0.225
d (fm)	0.25	0.30	0.25	0.30	0.27	0.18
ℓ_0	10	10	10	20	10	20
$\phi \ell_0$ (Deg.)	1.5	10	2.5	22.5	1.5	2.5
D_0	0.5	0.5	2	0.5	1.5	3.5
Γ_0	5.3	5.3	5.3	5.3	10.3	6.3
ℓ_g	10	11	10	11	11	10
Δ	0.687	0.681	0.50	0.68	0.45	0.492
R (fm)	7.88	8.43	8.92	8.27	8.83	8.83
d/R	0.037	0.0355	0.0288	0.0362	0.025	0.0254
p	10.33	10.44	11.30	10.39	10.73	11.33
n	5.04	5.11	5.49	5.04	5.25	5.49
h	11.68	10.95	10.33	11.13	10.43	10.44
θ_R (Rad)	0.0933	0.0870	0.025	0.085	0.089	0.018
θ_{Nuc1} (Rad)	-0.0187	-0.0198	-0.027	-0.027	-0.0275	-0.0182
σ_r (mb) (GFM)	93.44	102.98	104.6	110.9	118.82	111.17
σ_r (mb) (FM)	87.02	89.57	104.20	103.56	113.09	122.71
χ^2	0.015	0.018	0.0140	0.017	0.15	0.015

The results show that the Fresnel features in the angular distribution which are obtained by the parameter p , it is noted that the parameter p decrease with the increase energy and increase with increase size of target All extracted values of parameters together other useful physical quantities are listed in Table 1.

CONCLUSION

We have analyzed the elastic scattering a particle by target nuclei $^4\text{He}+^{90}\text{Zr}$ (at laboratory energies 21, 23 and 25 MeV) and $^4\text{He}+^{91}\text{Zr}$ (at laboratory energies 21, 23.4 and 25 MeV) using combined model of McIntyre and Regge Model. There are two quantities determined type of diffraction pattern in the angular distribution the diffraction parameter kR (ℓ_g the angular momentum) and (the strength of the Coulomb interactions which represents by Somerfield parameter n . The radius interaction region R is increasing when the atomic mass of target nucleus is increased and decrease with increase energy with fix target the better formula of $R = r_0 A_T^{1/3} + r_0$. The diffusivity parameter d , the parameters ℓ_0 , $\phi\ell_0$, D_0 and Γ_0 used in backward angel has been obtained, ℓ_0 the orbital angular momentum which represent the location for the pole, the D_0 amplitude and the Γ_0 width exhibit the similar behavior the width of the pole, ϕ_0 which estimate the phase angel determined the size of oscillation (Istaiti, 2018).

ACKNOWLEDGEMENT

The researcher acknowledges Applied Science Private University, Amman, Jordan for the fully financial support granted of this research.

REFERENCES

- Badran, R.I. and A.I. Istaiti, 2016. Analysis of elastic scattering of $4\text{He}+^{58}\text{Ni}$ and $4\text{He}+^{60}\text{Ni}$ using semiclassical models. Proceedings of the 6th AIP International Conference on Advances in Applied Physics and Materials Science Congress and Exhibition (APMAS 2016) Vol. 1809, June 1-3, 2016, AIP Publishing, Istanbul, Turkey, pp: 020007-1-020007-7.
- Badran, R.I. and D.A. Masri, 2013. Analysis of diffractive features in elastic scattering of 7Li by different target nuclei at different energies. Proceedings AIP 3rd International Conference on Advances in Applied Physics and Materials Science Congress Vol. 1569, April 24-28, 2013, AIP, Antalya, Turkey, ISBN:978-0-7354-1197-5, pp: 81-85.
- Badran, R.I., A.I. Istaiti, W.N. Mashaqbeh and I.H. Al-Lehyani, 2015. Regge pole analysis of elastic scattering of α particles by even isotopes of Ni target nuclei at incident energies above Coulomb barrier. Intl. J. Mod. Phys. E., 24: 1550082-1-1550082-21.
- Badran, R.I., H. Badahdah, M. Arafah and R. Khalidi, 2010. Strong absorption analysis of elastic scattering reactions using McIntyre and Frahn-Venter models. Intl. J. Mod. Phys. E., 19: 2199-2217.
- Istaiti, A.I., 2018. Analysis of elastic scattering of particles on $^{70}, ^{72}, ^{74}, ^{76}\text{Ge}$ targets at $E_{\text{Lab}} = 25\text{MeV}$. Intl. J. App. Eng. Res., 13: 6193-6196.
- Badran, R.I. and A.I. Istaiti, 2016. Analysis of elastic scattering of $4\text{He}+^{58}\text{Ni}$ and $4\text{He}+^{60}\text{Ni}$ using semiclassical models. Proceedings of the 6th AIP International Conference on Advances in Applied Physics and Materials Science Congress and Exhibition (APMAS 2016) Vol. 1809, June 1-3, 2016, AIP Publishing, Istanbul, Turkey, pp: 020007-1-020007-7.